



SPE Paper #: 99326

## Supercritical CO<sub>2</sub> and H<sub>2</sub>S – Brine Drainage and Imbibition Relative Permeability Relationships for Intergranular Sandstone and Carbonate Formations

D. Brant Bennion, Hycal Energy Research Laboratories Ltd., Calgary, AB, Canada, and  
Stefan Bachu, Alberta Energy and Utilities Board, Edmonton, AB, Canada

Copyright 2006, Society of Petroleum Engineers

This paper was prepared for presentation at the SPE Europec/EAGE Annual Conference and Exhibition held in Vienna, Austria, 12–15 June 2006.

This paper was selected for presentation by an SPE Program Committee following review of information contained in an abstract submitted by the author(s). Contents of the paper, as presented, have not been reviewed by the Society of Petroleum Engineers and are subject to correction by the author(s). The material, as presented, does not necessarily reflect any position of the Society of Petroleum Engineers, its officers, or members. Papers presented at SPE meetings are subject to publication review by Editorial Committees of the Society of Petroleum Engineers. Electronic reproduction, distribution, or storage of any part of this paper for commercial purposes without the written consent of the Society of Petroleum Engineers is prohibited. Permission to reproduce in print is restricted to an abstract of not more than 300 words; illustrations may not be copied. The abstract must contain conspicuous acknowledgment of where and by whom the paper was presented. Write Librarian, SPE, P.O. Box 833836, Richardson, TX 75083-3836 U.S.A., fax 01-972-952-9435.

### Abstract

Sequestration of CO<sub>2</sub> and H<sub>2</sub>S (acid gas) in deep underground formations is a means for reducing atmospheric emissions of acid gas produced from sour gas reservoirs that has been practiced for 15 years in North America and that is currently being considered in other regions such as the Middle East and central Asia. Furthermore, acid-gas injection operations constitute a commercial-scale commercial analogue to CO<sub>2</sub> injection in geological media as a climate change mitigation measure. Deep saline aquifers provide a very large capacity for the sequestration of acid and greenhouse gases, being ubiquitous in all sedimentary basins around the world. Proper understanding of the relative permeability character of such systems is essential in ascertaining gas injectivity and migration, and in assessing the suitability, containment and safety of prospective injection sites.

Pure CO<sub>2</sub> and H<sub>2</sub>S represent the compositional end-members of acid and greenhouse gases, thus the interest in measuring their displacement properties. This paper presents the detailed experimental equipment and protocols, and the results of a series of relative permeability tests conducted at full reservoir conditions using supercritical pure CO<sub>2</sub> and H<sub>2</sub>S on samples of intercrystalline sandstone and carbonate rocks from the Wabamun Lake area in central Alberta, Canada, where large CO<sub>2</sub> sources and several acid-gas injection operations exist. Results for both drainage and imbibition relative permeability experiments are presented for each fluid and rock type, as well as measurements of the interfacial tension (IFT) between brines and CO<sub>2</sub> and H<sub>2</sub>S at in situ conditions, and correlations of these results with the IFT, measured rock capillary pressure, pore size distribution and mineralogical data. The results allow a comparison between the drainage and imbibition relative

permeability character and performance of the two gases, and provide a valuable dataset for the evaluation and simulation of acid gas disposal and CO<sub>2</sub> storage projects.

### Introduction

Deep gas reservoirs in Rocky Mountain foreland basins in Canada and the United States contain hydrogen sulphide (H<sub>2</sub>S) and carbon dioxide (CO<sub>2</sub>) that has to be removed in order to meet safety and market requirements. These gases are separated from the produced gas at gas plants usually using an amine-based process that results in sweet gas that is sent to markets and a concentrated stream of acid gas (a mixture of H<sub>2</sub>S and CO<sub>2</sub> with other gases present in small concentrations). Because sweetening the acid gas is costly in a weak, depressed sulphur market, and sulphur stored on site constitutes a liability, more and more upstream and midstream companies in North America are turning to acid gas disposal by injection into deep into depleted oil or gas reservoirs, or saline aquifers<sup>1</sup>. Regulatory constraints that, since 1989, do not allow flaring of acid gas from gas plants with an output greater than 1 t/d, combined with economic conditions, led to an increase in the number of acid-gas injection operations in western Canada from one in 1990 to more close to 50 today. Dry acid gas is injected in a dense-fluid (liquid or supercritical) state at depths that vary between ~1000 and ~3400 m in both carbonate and siliciclastic formations whose porosity is generally less than 12% and permeability in the order of milliDarcies to tens of milliDarcies. In approximately 60% of the cases, the acid gas is injected into deep aquifers, whose salinity ranges from 20,000 ppm to 340,000 ppm. Figure 1 illustrates the location of these operations in Alberta and British Columbia, and detailed characterizations of these operations are provided elsewhere<sup>2, 3</sup>. Similarly, close to 20 acid-gas injection operations are currently active in the United States, most of them in Wyoming, Oklahoma and Texas, with the largest operation in the world being operated by ExxonMobil at the LaBarge field in Wyoming. As sour reservoirs are being produced in the Arabian Gulf and central Asia, producers in Iran, the Arab Emirates and Kazakhstan are also turning to acid gas disposal by deep injection, and it is likely that this practice will increasingly be used around the world. Additionally, geological storage in hydrocarbon reservoirs and deep saline aquifers of CO<sub>2</sub> captured at large plants has been recently recognized as a possible mitigation

measure for reducing atmospheric emissions of greenhouse gases with large potential for being used this century<sup>4, 5</sup>. Geological storage in deep saline aquifers of CO<sub>2</sub> produced from gas reservoirs occurs already at Sleipner in the North Sea (operated by Statoil) and at In Salah in Algeria (operated by BP), and is planned at several other places around the world like Gorgon Island in northwestern Australia (operated by Chevron).

In both cases of deep injection of acid and greenhouse gases into depleted hydrocarbon reservoirs or deep saline aquifers there is need to know the characteristics of the displacement process involving the injected gas and in situ fluids, the most important being relative permeability and residual gas saturation. Another potential application for these data is when CO<sub>2</sub> or acid gas is injected into a conventional oil reservoir for EOR purposes where bottom water is present or water is co-injected or alternated with the injected CO<sub>2</sub> or acid gas in a WAG process for mobility control. This is because these characteristics affect injectivity and flow rate, spread of the plume of the injected gas, and residual trapping of gas in the pore space<sup>6</sup>. Capillary pressure is another important parameter, particularly for caprock, to ensure that the injection pressure is maintained at all times below the threshold entry pressure to ensure long term containment of the injected gas. However, such data are available only for CO<sub>2</sub>-oil systems as a result of the use of CO<sub>2</sub> for enhanced oil recovery, mostly in the Permian basin in west Texas. No data are publicly available for CO<sub>2</sub>-brine systems or for H<sub>2</sub>S-brine systems, the two constituting the end members of acid gas mixtures.

To cover this gap in data and knowledge, the authors commenced an experimental program in 2004 of testing the displacement characteristics at in situ conditions of these two gases on core plugs taken from various siliciclastic and carbonate formations in the Wabamun Lake area southwest of Edmonton in Alberta, western Canada. Several acid-gas injection operations are currently active in this region. In addition, major coal-fired power plants, refineries and petrochemical plants are located in this same area, with the potential in the future of capturing CO<sub>2</sub> emitted at these large stationary sources and injecting it deep into geological media to reduce CO<sub>2</sub> atmospheric emissions. The in situ conditions and rock characteristics for these tests are representative not only for the Edmonton region, but for the entire Alberta basin, and likely for all Rocky Mountain foreland basins in North America and similar basins elsewhere.

Multiple samples were taken from several formations in the Wabamun Lake area, providing four distinct sandstone, one shale and five carbonate data sets. The pore characteristics, capillary pressure, interfacial tension (IFT) and relative permeability results for CO<sub>2</sub> displacing brine (drainage) were reported previously<sup>7, 8</sup>. This paper reports the results for both CO<sub>2</sub> and H<sub>2</sub>S displacing brine (drainage) and then subsequently being displaced by it (imbibition) for new core samples from the sandstone Viking Formation (well 16-33-48-1W5) and the carbonate Nisku Formation (well 4-14-51-4W5). These Viking and Nisku rock samples were tested at the same in-situ conditions of temperature, pressure and brine

salinity as the corresponding Viking and Nisku samples tested initially<sup>7</sup>, to assess the effect of rock properties. This paper is the third in the series describing this research program and the reader is referred to the first paper<sup>7</sup> for details regarding the geological setting and the equipment and procedures used to conduct the relative permeability measurements, and to the second paper<sup>8</sup> for the specific details for the high-pressure air-mercury capillary pressure and IFT measurements at reservoir conditions.

The only variance in the procedures for this set of experiments was the use of pure H<sub>2</sub>S as the displacement fluid for the comparative tests. Due to the highly toxic and corrosive nature of H<sub>2</sub>S, special coreholder cells, pumps and displacement equipment (composed of Hastalloy C or Titanium) were required and the tests were conducted in an automated explosion-proof isolation laboratory at Hycal Energy Laboratories Ltd. for safety purposes.

## Experimental Results

Table 1 provides a summary of the location and pore characteristics of the Viking and Nisku formation core samples which were used in this test program. Table 2 summarizes the in-situ test conditions and the measured interfacial tension between CO<sub>2</sub> or H<sub>2</sub>S and equilibrium brine at reservoir conditions (IFT measured by drop pendant interfacial tensiometer<sup>8</sup>). Examination of the interfacial tension data contained in Table 2 indicates that, for the same conditions of temperature, pressure and salinity, dense-phase H<sub>2</sub>S exhibits significantly lower IFT with its equilibrium H<sub>2</sub>S-saturated brine than supercritical CO<sub>2</sub> (typically in the range of approximately 35-40% of the CO<sub>2</sub>-brine IFT values). This lower interfacial tension can be attributed to the great solubility of H<sub>2</sub>S in brine in comparison to CO<sub>2</sub> and has the effect of a significant reduction in the capillary pressure of the H<sub>2</sub>S-brine system compared with the CO<sub>2</sub>-brine system at in-situ conditions (Figures 2b and 3b).

Table 3 provides a summary of the endpoint permeability values and terminal fluid saturation values that were measured for the drainage and imbibition floods conducted with CO<sub>2</sub> and H<sub>2</sub>S on the Viking and Nisku core samples. An initial permeability to CO<sub>2</sub>- or H<sub>2</sub>S-saturated brine was determined at a condition of 100% water saturation (primary imbibition) for both sets of samples. This was followed by an unsteady-state displacement with either gas (CO<sub>2</sub> and H<sub>2</sub>S) until the maximum gas saturation and a stabilized endpoint permeability to the gas were obtained (primary drainage displacement). The drainage cycle was then followed by gas-saturated brine displacing the mobile gas phase (CO<sub>2</sub> or H<sub>2</sub>S) from the sample until a trapped gas saturation was achieved and the permeability to equilibrium brine at the trapped gas saturation was measured (secondary imbibition displacement). Both CO<sub>2</sub> and H<sub>2</sub>S drainage and imbibition displacements were conducted on both the Viking and Nisku cores to facilitate direct comparison between the two gases. Due to the higher solubility and more aggressive potential nature of the H<sub>2</sub>S-brine system, the CO<sub>2</sub> displacements were conducted first, followed by cleaning of the core and subsequent resaturation and commencement of the H<sub>2</sub>S-based tests.

Figures 2a and 2b show, respectively, the pore size distribution profile and converted capillary pressure curves for CO<sub>2</sub> and H<sub>2</sub>S - brine at reservoir conditions for the Viking Formation sandstone sample. It can be noted in Figure 2a that the Viking sample exhibits a right skewed pore size distribution with a large fraction of pore throats centered around the 10 micron range, with a trailing edge of microporosity (likely mostly contained in interstitial clay and leached grain remnants). Tables 4 and 5, and Figures 2c and 2d present the drainage and imbibition relative-permeability curves for CO<sub>2</sub> and H<sub>2</sub>S, respectively, displacing and being displaced by brine in the Viking Fm. sandstone rock sample. Hysteresis effects (a variance in the value of the relative permeability between the drainage – i.e., water saturation decreasing, and imbibition – i.e. water saturation increasing, tests) are evident in Figures 2c and 2d and are relatively comparable for the gas phase between the CO<sub>2</sub> and H<sub>2</sub>S tests (slightly less pronounced for H<sub>2</sub>S than CO<sub>2</sub>, consistent with the lower IFT of the H<sub>2</sub>S-brine system). There is considerably more hysteresis between the H<sub>2</sub>S and CO<sub>2</sub> tests for the brine relative-permeability curves, with markedly more hysteresis present in the H<sub>2</sub>S case. The residual trapped gas saturation in the H<sub>2</sub>S tests was considerably lower than in the CO<sub>2</sub> test for the Viking sample. This is consistent with the expectation that, with the lower IFT, capillary forces should be reduced, resulting in a reduction in capillary-induced residual-gas saturation effects. This effect may also be related to better conformance due to the lower permeability of the injected brine phase, which has resulted in more effective sweep (less bypassing) of the pore system. The lower endpoint relative permeability for the H<sub>2</sub>S-saturated brine phase in comparison to the CO<sub>2</sub>-saturated brine phase, however, is not consistent with this lower trapped gas saturation, as one would expect to have an increased brine phase relative permeability value at a lower trapped gas saturation. Normally it would also be expected that, during the imbibition cycle, the brine-phase relative-permeability values would be comparable or greater than those observed for the drainage cycle. This is the case for the CO<sub>2</sub> test, but the brine-phase relative permeability is considerably lower in the H<sub>2</sub>S imbibition flood than in the corresponding CO<sub>2</sub> one. It was postulated that the low pH of the H<sub>2</sub>S-saturated brine system may be reacting with soluble calcite-based cements in the Viking pore system, potentially releasing insoluble fines or particulates that may have been embedded and previously stabilized by the low pH soluble cement material. The mobilized fines or particulates may have plugged some pore throats during the drainage cycle, with the effect of reduced permeability. Figure 3 illustrates the pre- and post-test scanning electron microscope (SEM) analysis of the Viking Formation samples. The dissolution and migration of clays is clearly evident between the pre- and post-test samples, as well as the creation of calcite-based precipitates that block portions of the pore system, precipitates that are believed to have been sourced from liberated calcite from low pH induced acid brine reactions in the sample matrix.

Figures 4a and 4b show, respectively, the pore size distribution profile and converted capillary pressure curves for CO<sub>2</sub> and H<sub>2</sub>S - brine at reservoir conditions for the Nisku Formation carbonate sample. It can be noted in Figure 4a that

the Nisku Fm. sample exhibits a much wider pore throat size distribution than the previous Viking Fm. sample, with considerably more pore throats in the micropore (<1 micron) range. Tables 6 and 7, and Figures 4c and 4d present the drainage and imbibition relative-permeability curves for CO<sub>2</sub> and H<sub>2</sub>S, respectively, displacing and being displaced by brine in the Nisku Fm. carbonate rock sample. Relative permeability hysteresis is, once again, relatively comparable for the gas phase between the CO<sub>2</sub> and H<sub>2</sub>S tests (again slightly less pronounced for H<sub>2</sub>S than CO<sub>2</sub>, consistent with the lower IFT of the H<sub>2</sub>S-brine system). There is considerably more hysteresis between the brine relative permeability curves between the H<sub>2</sub>S and CO<sub>2</sub> tests, but in this case the hysteresis is more evident in the higher-IFT CO<sub>2</sub> displacement test (as would be expected) and the relative permeability values to brine are higher than in the drainage case, once again more consistent with general expectations. This more conventional behavior suggests that limited or no damage to the pore system was caused by the acid-brine reaction in the much more soluble (and uniform) Nisku carbonate matrix, with potentially even some permeability enhancement. Figure 5 illustrates the pre- and post-test SEM analysis of the Nisku Fm. sample which was conducted to verify this supposition. Other than some minor dissolution effects on the carbonate matrix, very little difference in the pore system is apparent when comparing the pre and post gas exposure samples, confirming the hypothesis.

Figures 6a and 6b directly compare the CO<sub>2</sub> and H<sub>2</sub>S drainage and imbibition displacements for the Viking Fm. core material, and Figures 6c and 6d provide a similar comparison for the Nisku Fm. core material. The data indicate that, in general, we see considerably greater hysteresis effects for both CO<sub>2</sub> and H<sub>2</sub>S on the secondary imbibition phase than we observe on the drainage phase. It can also be observed that, in both rock types, maximum gas saturation obtained with H<sub>2</sub>S is slightly lower than obtained with CO<sub>2</sub> on the primary drainage cycles. This is somewhat counterintuitive, as it would be expected that the lower-IFT H<sub>2</sub>S system should be more effective at displacing the brine to a lower residual saturation than the CO<sub>2</sub>. In all cases it can be observed that the gas relative permeability value for H<sub>2</sub>S is greater than that for CO<sub>2</sub> (during both drainage and imbibition cycles). It may be that the higher mobility of the gas in the H<sub>2</sub>S displacements is counteracting the lower IFT, resulting in more macroscopic bypassing of the pore system, leading to higher trapped-water saturations in the H<sub>2</sub>S tests in contrast to the CO<sub>2</sub> displacements.

## Conclusions

This paper has presented and summarized the characteristics of CO<sub>2</sub> and H<sub>2</sub>S displacing brine at in situ conditions for a sandstone and carbonate formation in the Wabamun Lake area of central Alberta, western Canada. The test results indicate that;

1. At comparable conditions of temperature, pressure and salinity, the IFT of H<sub>2</sub>S-brine systems is about 35-40% of that of CO<sub>2</sub> brine systems.

2. The H<sub>2</sub>S-saturated brines were much more aggressive in reacting with the rock than the CO<sub>2</sub>-saturated brines. In the almost completely acid soluble Nisku carbonate test, permeability enhancements were observed. In the Viking sandstone tests, the dissolution of carbonate cements released previously stabilized silicate fines, which migrated and reduced the permeability of the pore system, making direct comparison of the CO<sub>2</sub> and H<sub>2</sub>S test results difficult due to the damage effect.
3. Basing the results on the undamaged Nisku Fm. carbonate facies, it appears that the lower IFT of the H<sub>2</sub>S-brine system results in improved ease of displacement (greater relative permeability to H<sub>2</sub>S in either a primary drainage or secondary imbibition mode).
4. Maximum supercritical gas saturation appears to be slightly less for the H<sub>2</sub>S than CO<sub>2</sub> displacements, possibly due to more macroscopic channeling and bypass effects due to the lower IFT and greater apparent mobility of the injected H<sub>2</sub>S gas in comparison to CO<sub>2</sub>.
5. In the absence of damage effects associated with acid brine reactions, the lower-IFT H<sub>2</sub>S displacements appear to exhibit much less hysteresis between drainage and imbibition than the CO<sub>2</sub> displacements. The variance in the relative permeability character between CO<sub>2</sub> and H<sub>2</sub>S appears to be more pronounced on secondary imbibition than during primary drainage.
6. Additional test data on other rock types containing less potential for damage/reactivity by the acid gas will be useful in expanding the existing dataset.

### Acknowledgements

The authors wish to express appreciation to the Alberta Energy and Utilities Board for permission to present these data, and to Donna Leach and Dan Magee for their assistance in the preparation of the manuscript and figures.

### References

1. Connock, L., Acid gas injection reduces sulphur burden. *Sulphur*, v. 272, 35-41, 2001.
2. Bachu, S., and W.D. Gunter, Overview of acid-gas injection operations in western Canada. Proceedings of 7th International Conference on Greenhouse Gas Control Technologies. *Volume 1: Peer-Reviewed Papers and Overviews* (E.S.Rubin, D.W.Keith and C.F.Gilboy, eds.), Elsevier, p. 443-448, 2005.
3. Bachu, S., and K. Haug, In-situ characteristics of acid-gas injection operations in the Alberta basin, western Canada: Demonstration of CO<sub>2</sub> geological storage. Carbon Dioxide Storage in Deep Geologic Formations – Results from the CO<sub>2</sub> Capture Project, Volume 2: *Geologic Storage of Carbon Dioxide with Monitoring and*

*Verification* (S. M. Benson, ed.), Elsevier, London, U.K., p 867-876, 2005.

4. International Energy Agency, *Prospects for CO<sub>2</sub> Capture and Storage*, IEA/OECD, Paris, France, 249 p., 2004.
5. Intergovernmental Panel on Climate Change, *IPCC Special Report on Carbon Dioxide Capture and Storage* (eds. B. Metz, O. Davidson, H.C. de Coninck, M. Loos and L.A. Mayer), Cambridge University Press, Cambridge, U.K., and New York, NY, U.S.A., 442 p., 2005.
6. Kumar, A., Noh, M., Pope, G.A., Sepehrnoori, K., Bryant, S., and Lake, L.W., Reservoir simulation of CO<sub>2</sub> storage in deep saline aquifers; Paper SPE 89343, 10 p., presented at the SPE/DOE Fourteenth Symposium on Improved Oil Recovery, Tulsa, OK, USA, April 17-21, 2004.
7. Bennion, B., and Bachu, S., Relative permeability characteristics for CO<sub>2</sub> displacing water in a variety of potential sequestration zones in the Western Canada Sedimentary Basin; Paper SPE 95547, 15 p., presented at the 2005 SPE Technical Conference and Exhibition, Dallas, TX, October 9-12, 2005.
8. Bennion, B., and Bachu, S., The impact of interfacial tension and pore size distribution/capillary pressure character on CO<sub>2</sub> relative permeability at reservoir conditions in CO<sub>2</sub>-brine systems; Paper SPE 99325, 10 p., presented at the SPE/DOE Fifteenth Symposium on Improved Oil Recovery, Tulsa, OK, USA, April 22-26, 2004.

Formation	Lithology	Well	Depth (m)	%Micro Pores (<1 $\mu\text{m}$ )	%Meso Pores	%Macro Pores (>3 $\mu\text{m}$ )	Mean Pore Throat Size ( $\mu\text{m}$ )	Porosity (%)
Viking	Sandstone	16-33-48-1 W5M	1342.46	27.6	7.6	64.8	10.76	19.5
Nisku	Carbonate	04-14-51-4 W5M	1952.77	33.2	18.8	48.0	4.32	11.4

Table 1 – Location and pore characteristics of the rock samples from the Wabamun Lake area, Alberta, Canada, tested in this study.

Formation	Pressure (MPa)	Temperature ( $^{\circ}\text{C}$ )	Brine Salinity (ppm)	IFT to $\text{CO}_2$ (mN·m)	IFT to $\text{H}_2\text{S}$ (mN·m)
Viking	8.6	35	28,286	32.12	12.2
Nisku	17.4	56	136,817	34.56	12.3

Table 2 – In-situ characteristics of formation water for the tests conducted in this study and the measured interfacial tension (IFT) between brine and  $\text{CO}_2$  and  $\text{H}_2\text{S}$  at these conditions.

Formation	Gas	Absolute Permeability to Brine (mD)	Drainage		Imbibition	
			Maximum Gas Saturation $S_{g\text{max}}$ (Fraction)	Maximum Gas Permeability at $S_{\text{wir}}$ (mD)	Trapped Gas Saturation $S_{\text{gir}}$ (Fraction)	Max. Brine Permeability at $S_{\text{gir}}$ (mD)
Viking	$\text{CO}_2$	21.72	0.577	5.73	0.297	7.92
	$\text{H}_2\text{S}$	22.02	0.519	4.91	0.159	2.89
Nisku	$\text{CO}_2$	21.02	0.508	2.10	0.218	11.56
	$\text{H}_2\text{S}$	17.75	0.455	3.96	0.265	4.41

Table 3 – Displacement characteristics for brine and  $\text{CO}_2$  or  $\text{H}_2\text{S}$  systems for sandstone and carbonate rock samples from the Wabamun Lake area, Alberta, Canada.

a.

CO <sub>2</sub> Saturation Fraction	Krg	Krw
0.000	0.0000	1.0000
0.029	0.0002	0.9150
0.058	0.0006	0.8332
0.087	0.0015	0.7546
0.115	0.0031	0.6794
0.144	0.0055	0.6076
0.173	0.0090	0.5392
0.202	0.0138	0.4743
0.231	0.0199	0.4130
0.260	0.0276	0.3553
0.289	0.0370	0.3014
0.317	0.0484	0.2512
0.346	0.0619	0.2050
0.375	0.0776	0.1628
0.404	0.0957	0.1248
0.433	0.1163	0.0912
0.462	0.1398	0.0622
0.490	0.1660	0.0380
0.519	0.1954	0.0190
0.548	0.2279	0.0059
0.577	0.2638	0.0000

b.

CO <sub>2</sub> Saturation Fraction	Krw	Krg
0.577	0.0000	0.2638
0.563	0.0010	0.2152
0.549	0.0036	0.1737
0.535	0.0079	0.1386
0.521	0.0141	0.1091
0.507	0.0220	0.0846
0.493	0.0317	0.0645
0.479	0.0432	0.0483
0.465	0.0566	0.0354
0.451	0.0719	0.0253
0.437	0.0890	0.0176
0.423	0.1080	0.0119
0.409	0.1288	0.0077
0.395	0.1516	0.0048
0.381	0.1763	0.0029
0.367	0.2029	0.0017
0.353	0.2314	0.0009
0.339	0.2618	0.0005
0.325	0.2941	0.0003
0.311	0.3284	0.0001
0.297	0.3646	0.0000

Table 4 – Measured relative permeability to CO<sub>2</sub> and equilibrium brine at in-situ conditions for a sample from the Viking Fm. sandstone from the Wabamun Lake area, Alberta, Canada: a) drainage, and b) imbibition.

a.

H <sub>2</sub> S Saturation Fraction	Krg	Krw
0.000	0.0000	1.0000
0.026	0.0001	0.9103
0.052	0.0004	0.8245
0.078	0.0011	0.7426
0.104	0.0022	0.6646
0.130	0.0040	0.5905
0.156	0.0065	0.5205
0.182	0.0101	0.4545
0.208	0.0149	0.3927
0.234	0.0209	0.3350
0.260	0.0285	0.2815
0.285	0.0377	0.2322
0.311	0.0488	0.1873
0.337	0.0618	0.1469
0.363	0.0770	0.1110
0.389	0.0945	0.0797
0.415	0.1145	0.0532
0.441	0.1372	0.0317
0.467	0.1628	0.0153
0.493	0.1913	0.0045
0.519	0.2230	0.0000

b.

H <sub>2</sub> S Saturation Fraction	Krw	Krg
0.519	0.0000	0.2230
0.501	0.0027	0.1774
0.483	0.0066	0.1394
0.465	0.0112	0.1081
0.447	0.0163	0.0827
0.429	0.0218	0.0622
0.411	0.0276	0.0459
0.393	0.0336	0.0332
0.375	0.0400	0.0235
0.357	0.0466	0.0162
0.339	0.0534	0.0109
0.321	0.0604	0.0071
0.303	0.0677	0.0045
0.285	0.0750	0.0027
0.267	0.0826	0.0016
0.249	0.0903	0.0010
0.231	0.0982	0.0006
0.213	0.1063	0.0004
0.195	0.1144	0.0002
0.177	0.1228	0.0001
0.159	0.1312	0.0000

Table 5 – Measured relative permeability to H<sub>2</sub>S and equilibrium brine at in-situ conditions for a sample from the Viking Fm. sandstone from the Wabamun Lake area, Alberta, Canada: a) drainage, and b) imbibition.

a.

CO <sub>2</sub> Saturation Fraction	Krg	Krw
0.000	0.0000	1.0000
0.025	0.0000	0.8698
0.051	0.0001	0.7509
0.076	0.0002	0.6429
0.102	0.0003	0.5454
0.127	0.0004	0.4578
0.152	0.0007	0.3798
0.178	0.0011	0.3108
0.203	0.0019	0.2504
0.229	0.0029	0.1981
0.254	0.0046	0.1533
0.279	0.0069	0.1157
0.305	0.0100	0.0845
0.330	0.0143	0.0594
0.356	0.0198	0.0396
0.381	0.0270	0.0247
0.406	0.0362	0.0141
0.432	0.0476	0.0070
0.457	0.0618	0.0028
0.483	0.0790	0.0008
0.508	0.0999	0.0000

b.

CO <sub>2</sub> Saturation Fraction	Krw	Krg
0.508	0.0000	0.0999
0.493	0.0011	0.0800
0.479	0.0042	0.0633
0.464	0.0096	0.0495
0.450	0.0176	0.0381
0.435	0.0281	0.0289
0.421	0.0414	0.0215
0.406	0.0575	0.0157
0.392	0.0765	0.0112
0.377	0.0985	0.0078
0.363	0.1234	0.0053
0.348	0.1515	0.0035
0.334	0.1827	0.0022
0.319	0.2171	0.0014
0.305	0.2546	0.0008
0.290	0.2955	0.0005
0.276	0.3396	0.0003
0.261	0.3871	0.0002
0.247	0.4380	0.0001
0.232	0.4923	0.0000
0.218	0.5500	0.0000

Table 6 – Measured relative permeability to CO<sub>2</sub> and equilibrium brine at in-situ conditions for a sample from the Nisku Fm. carbonate from the Wabamun Lake area, Alberta, Canada: a) drainage, and b) imbibition.

a.

H <sub>2</sub> S Saturation Fraction	Krg	Krw
0.000	0.0000	1.0000
0.023	0.0001	0.9168
0.046	0.0002	0.8367
0.068	0.0003	0.7595
0.091	0.0005	0.6855
0.114	0.0006	0.6146
0.137	0.0008	0.5469
0.159	0.0011	0.4825
0.182	0.0016	0.4214
0.205	0.0025	0.3638
0.228	0.0041	0.3097
0.250	0.0066	0.2593
0.273	0.0105	0.2125
0.296	0.0166	0.1697
0.319	0.0256	0.1309
0.341	0.0385	0.0963
0.364	0.0569	0.0662
0.387	0.0822	0.0409
0.410	0.1167	0.0208
0.432	0.1626	0.0066
0.455	0.2231	0.0000

b.

H <sub>2</sub> S Saturation Fraction	Krw	Krg
0.455	0.0000	0.2231
0.446	0.0002	0.2023
0.436	0.0009	0.1824
0.427	0.0023	0.1635
0.417	0.0045	0.1457
0.408	0.0078	0.1288
0.398	0.0122	0.1129
0.389	0.0178	0.0980
0.379	0.0248	0.0841
0.370	0.0332	0.0713
0.360	0.0432	0.0595
0.351	0.0549	0.0487
0.341	0.0683	0.0389
0.332	0.0836	0.0302
0.322	0.1008	0.0225
0.313	0.1200	0.0160
0.303	0.1412	0.0105
0.294	0.1646	0.0061
0.284	0.1903	0.0029
0.275	0.2182	0.0008
0.265	0.2485	0.0000

Table 7 – Measured relative permeability to H<sub>2</sub>S and equilibrium brine at in-situ conditions for a sample from the Nisku Fm. carbonate from the Wabamun Lake area, Alberta, Canada: a) drainage, and b) imbibition.



Figure 1 – Location of acid-gas injection operations in Canada.

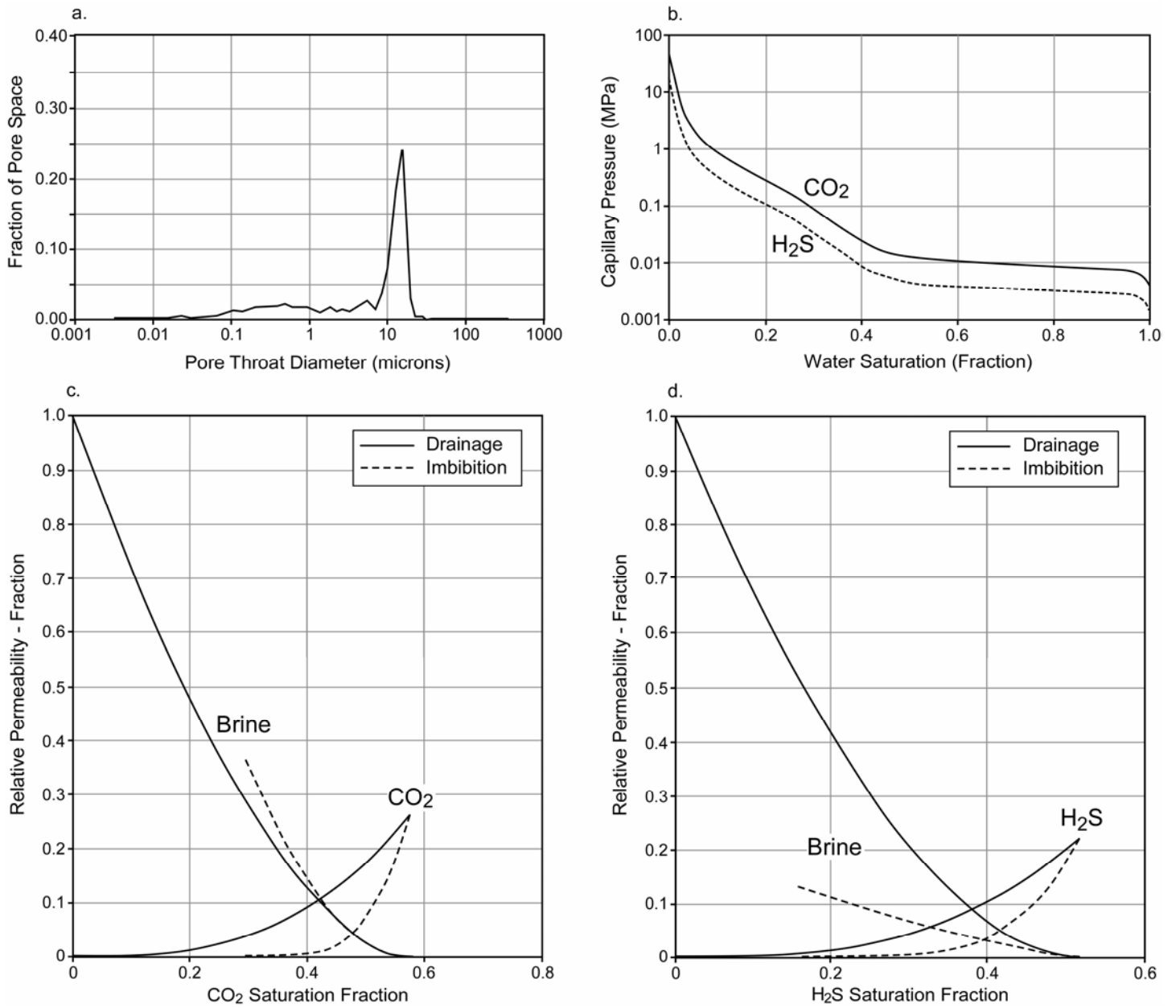


Figure 2 – Displacement characteristics of acid gas-brine systems for the sandstone Viking Fm. in the Edmonton area of central Alberta, Canada: a) pore size, b) capillary pressure, c) relative permeability for CO<sub>2</sub>-brine, and d) relative permeability for H<sub>2</sub>S-brine.

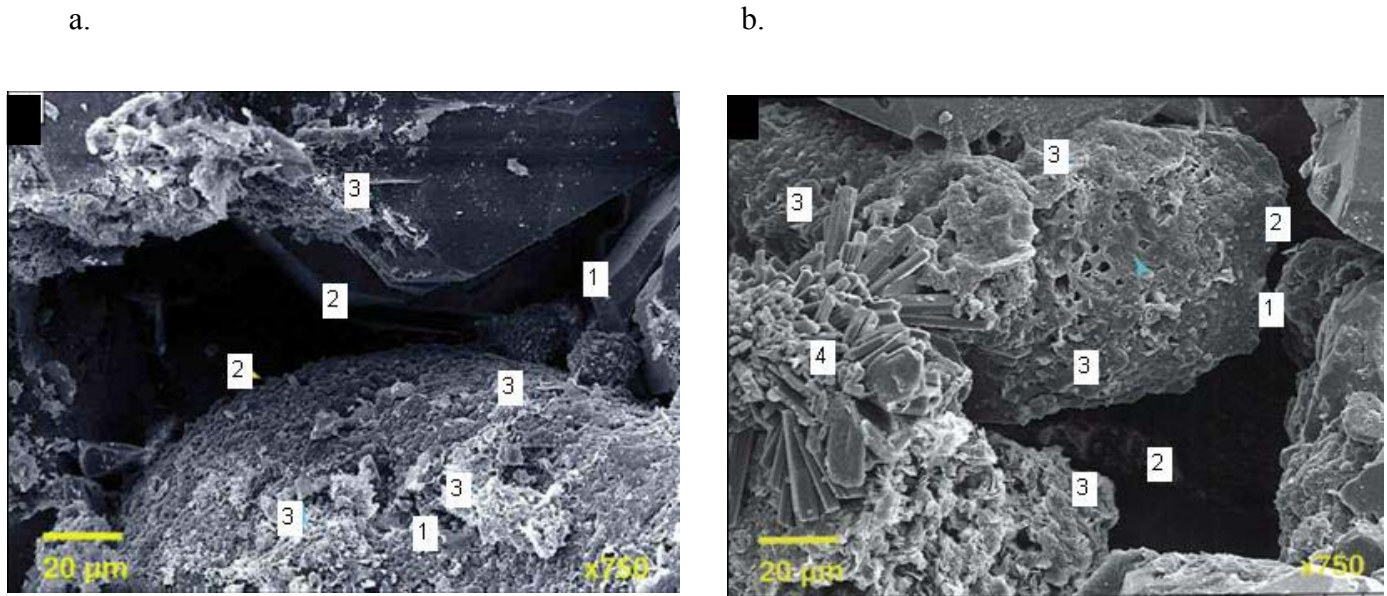


Figure 3 - Petrographic SEM analysis of Viking Fm. sandstone samples: a) pre-test, and b) post test after flooding with CO<sub>2</sub> and H<sub>2</sub>S. The numbers on the images indicate: (1) - quartz overgrowths, (2) - intergranular porosity, (3) - leached and migrated grain coating clays and (4) - blocking precipitated calcite crystal.

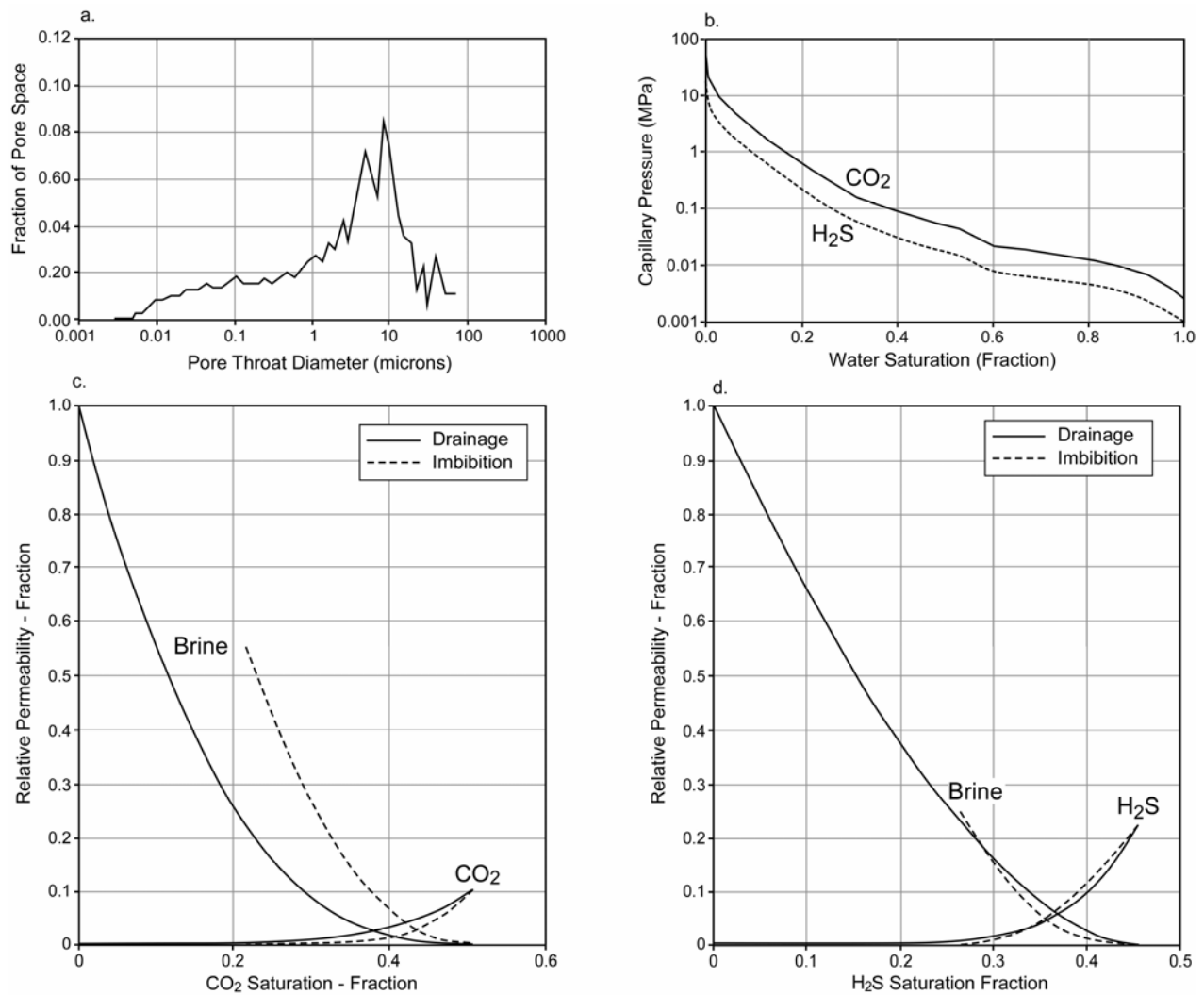


Figure 4 – Displacement characteristics of acid gas-brine systems for the sandstone Nisku Fm. in the Edmonton area of central Alberta, Canada: a) pore size, b) capillary pressure, c) relative permeability for CO<sub>2</sub>-brine, and d) relative permeability for H<sub>2</sub>S-brine.

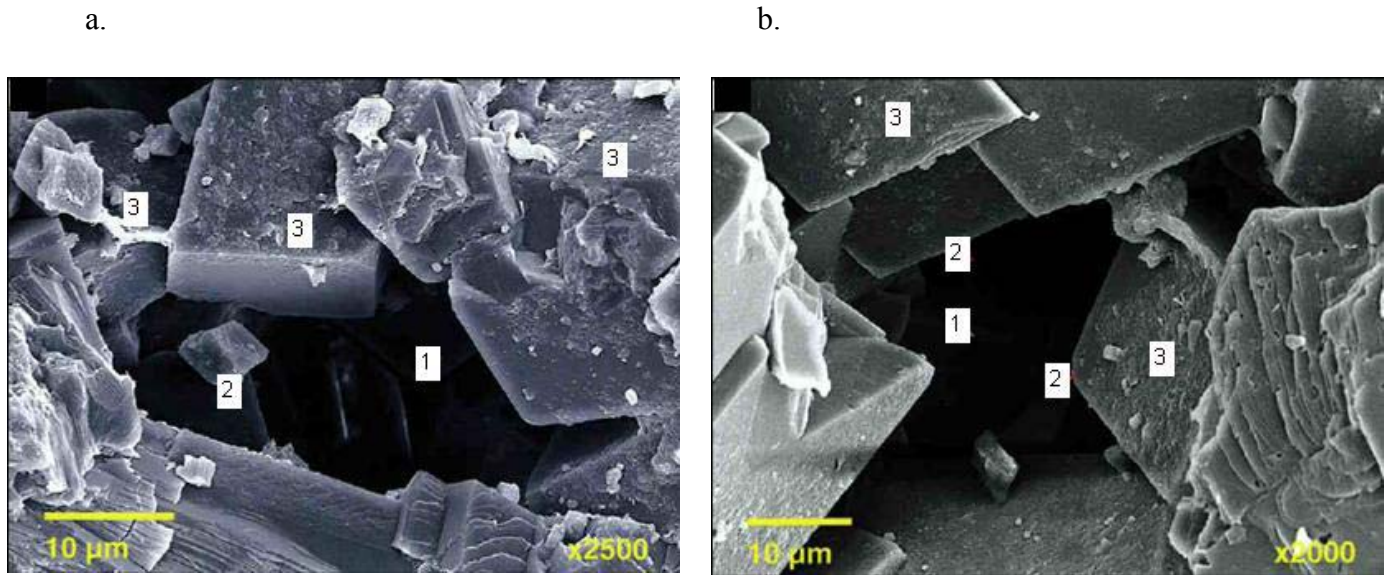


Figure 5 - Petrographic SEM analysis of Nisku Fm. carbonate samples: a) pre-test, and b) post-test after flooding with CO<sub>2</sub> and H<sub>2</sub>S. The numbers on the images indicate: (1) - intergranular porosity, (2) - dolomite cement, (3) - residual trace drilling mud fines.

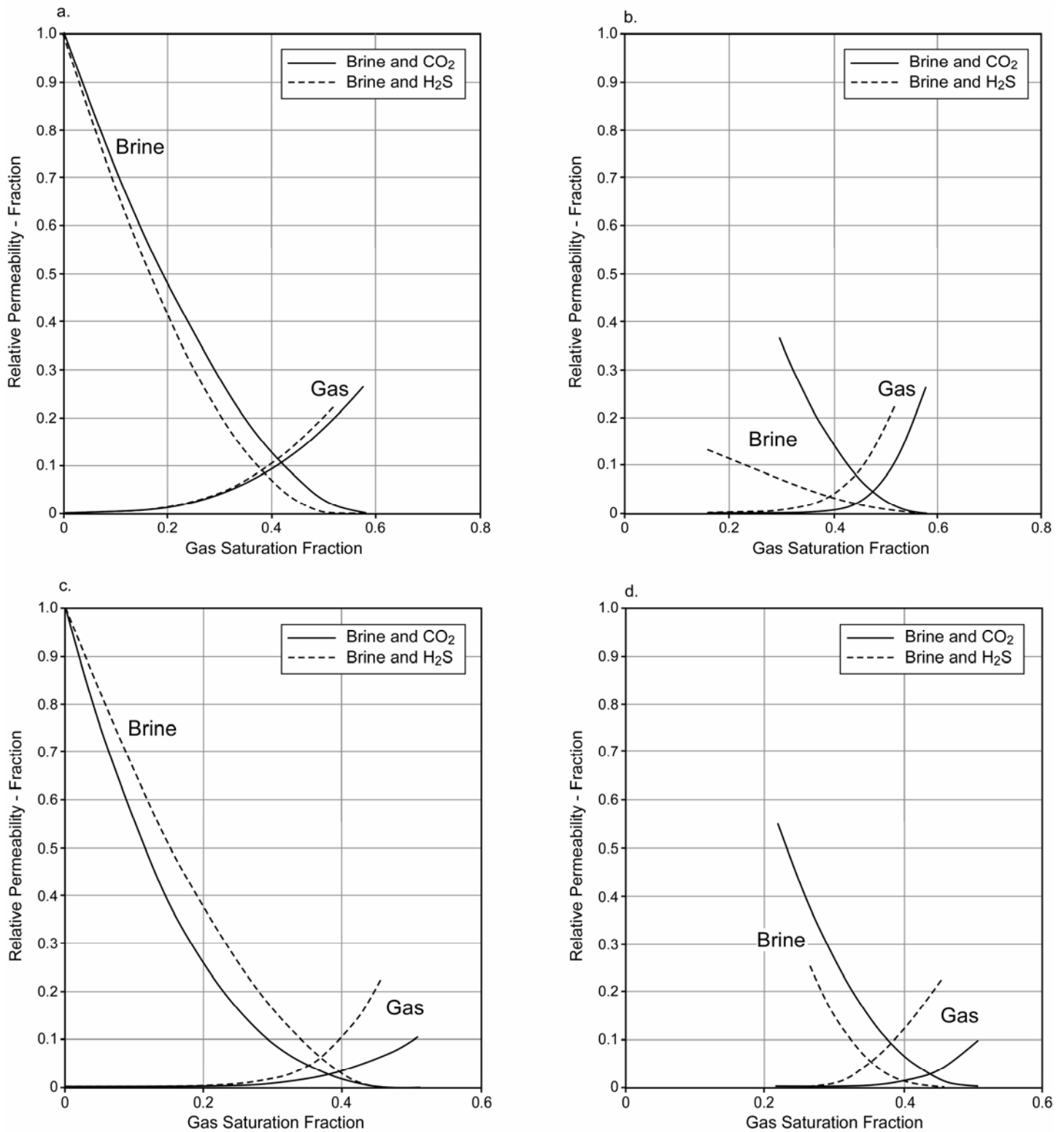


Figure 6 – Comparison between relative permeability for CO<sub>2</sub>-brine and H<sub>2</sub>S-brine systems for: a) drainage in the Viking Fm. sandstone; b) imbibition in the Viking Fm. sandstone, c) drainage in the Nisku Fm. carbonate; d) imbibition in the Nisku Fm. carbonate.